

# Phase control in multiexposure spatial frequency multiplication

Yong Zhao,<sup>a)</sup> Chih-Hao Chang, Ralf K. Heilmann, and Mark L. Schattenburg

Space Nanotechnology Laboratory, Massachusetts Institute of Technology, Cambridge, Massachusetts 02139

(Received 8 June 2007; accepted 4 September 2007; published 10 December 2007)

Multiexposure spatial frequency multiplication is a technique that allows the spatial frequency of grating patterns to be increased by integer factors 2,3,4,... by applying a nonlinear development process between patterning steps. One of the main technical issues with this technique is how to accurately place subsequent patterns on a substrate with respect to previously established patterns, which is referred to as phase control of the overlay. The authors report a technique that achieves accurate phase control over large areas during spatial frequency multiplication by utilizing a surrounding alignment grating. Three key factors—the angle, period, and phase of the alignment grating—have been accurately measured and utilized to position subsequent patterns with respect to previous patterns. Some factors that can dramatically diminish the accuracy of phase control, such as particle-induced substrate distortion and nonlinear distortion of the alignment grating, have also been considered and minimized in order to improve the accuracy of phase control. For spatial frequency doubling with a 574 nm principal pitch, the authors achieved overlay phase errors with a mean of  $-1.0 \text{ nm} \pm 2.8 \text{ nm}(1\sigma)$  between level 1 and level 2 grating patterns over a  $25 \times 32.5 \text{ mm}^2$  area. © 2007 American Vacuum Society. [DOI: 10.1116/1.2794318]

## I. INTRODUCTION

High spatial-frequency periodic patterns have many applications in various fields.<sup>1</sup> For example, high density patterns can be applied in nanomagnetism as magnetic storage media. In precision metrology, periodic patterns with fine pitch can be utilized as reference gratings. There are also important applications for high spatial-frequency patterns in nanophotonics.

For two-beam single-exposure interference lithography (IL), the period of the interference pattern is given by  $\lambda/(2n \sin \theta)$ , where  $\lambda$  is the photon wavelength,  $n$  is the refractive index of the lithography medium, and  $\theta$  is the incidence angle of the interfering beams. The maximum spatial frequency of a single-exposure grating pattern is  $2n/\lambda$ .<sup>2</sup> Higher spatial-frequency patterns can be fabricated by decreasing  $\lambda$  (e.g., by using shorter wavelength lasers) or increasing  $n$  (e.g., immersion lithography). However, these methods are both costly and have ultimate limits.

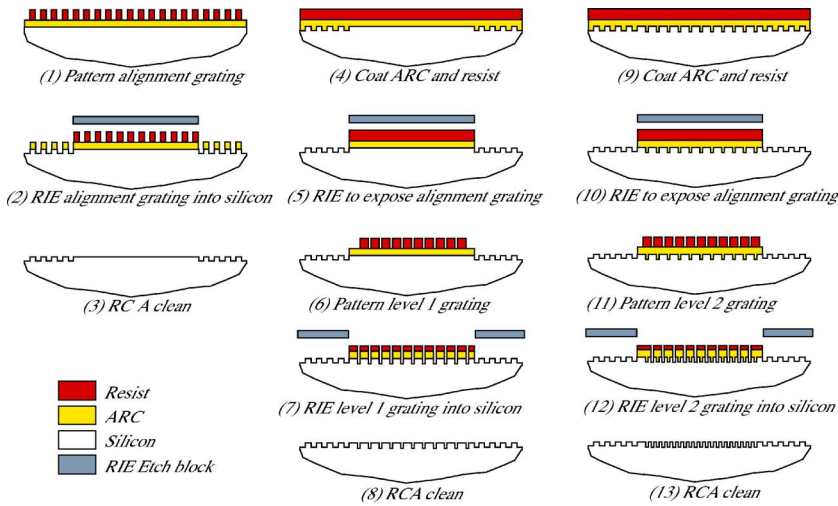
Spatial-frequency multiplication is an alternative method for achieving higher spatial-frequency patterns by interleaving new patterns among previous ones. At least three kinds of spatial-frequency multiplication techniques have been developed over the past 30 years. Near-field lithography multiplies the spatial frequency of mask grating patterns based on the near-field properties of grating diffraction.<sup>3,4</sup> Another technique is process-based spatial-frequency multiplication, which has been used to fabricate sub-200-nm pitch gratings.<sup>5,6</sup> Multiexposure spatial-frequency multiplication can extend the spatial frequency of patterns with integer factors 2,3,4,... by applying a pattern transfer process between exposures,<sup>7,8</sup> thanks to the nonlinearity of modern photoresists which provide a sharp threshold between exposed and

unexposed regions. Compared to previous techniques of multiplying the spatial frequency of IL-generated patterns, the technique reported here is able to perform spatial-frequency multiplication over large areas with small phase errors.

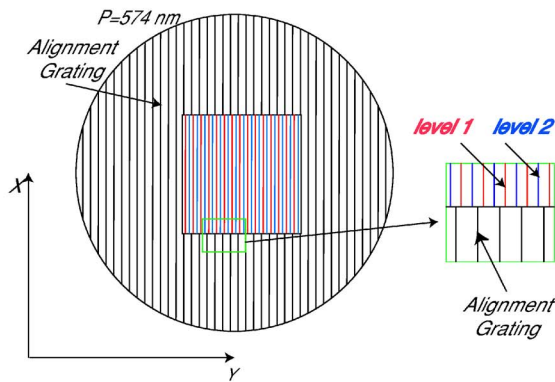
Figure 1(a) summarizes our process for achieving frequency doubling. The first step (1–3) is to form a grating pattern of pitch  $p$  in the outer areas of the photoresist, which is then developed and etched into the silicon substrate as the “alignment grating.” The wafer is then coated with a new antireflection coating (ARC) and photoresist in the central area. In the second step (4–8), after measuring the angle, period, and phase of the alignment grating, the level 1 pattern is placed on the substrate in the central area with the same grating angle and period as the alignment grating but with a certain phase shift. This pattern is then developed and etched into a silicon substrate. Afterwards new ARC and photoresist are spun in the central area. In the final step (9–13), we place the level 2 pattern with the same grating angle and period as the alignment grating, but with a different phase shift. Phase control of frequency doubling is schematically shown in Fig. 1(b). As shown in the enlarged window, the level 1 pattern has a  $\pi/2$  phase shift with respect to the alignment grating, and there is a  $3\pi/2$  phase shift between the level 2 pattern and the alignment grating. Therefore, we achieve a  $\pi$  phase shift between the level 1 and level 2 patterns in the central area, which means the spatial frequency of the original pattern is doubled. In this paper, we will focus on the phase control techniques crucial to spatial-frequency doubling. Details of the nanofabrication process will be reported separately.

Scanning-beam interference lithography (SBIL) (Refs. 1, 9, and 10) is utilized to generate grating patterns over large areas. The SBIL prototype tool, referred to as the Nanoruler, has been recently developed at MIT. The Nanoruler uses the

<sup>a)</sup>Electronic mail: yongzhao@mit.edu



(a) Spatial Frequency Doubling Processing Steps



(b) Phase Control of Spatial Frequency Doubling

interference fringes between two coherent laser beams to define highly coherent gratings in photoresist.<sup>10</sup> The substrate, sitting on an interferometer-controlled air-bearing stage, is stepped and scanned under the interference image (the interference image is much smaller than the whole desired patterning area) to expose large-area patterns. The Nanoruler allows the fabrication of grating patterns with a phase repeatability of a few nanometers.

Measuring the phase of the alignment grating is very important for correctly placing subsequent patterns on the substrate with respect to previous patterns. We use two phase detection schemes: homodyne and heterodyne reading modes (Fig. 2). For the homodyne reading mode, as shown in Fig. 2(a), the left and right interference arms, both modulated by 100 MHz, are incident upon the alignment grating. The superimposed reflected left arm and back-diffracted right arm are detected by a photodiode.<sup>9</sup> The voltage measurement of the photodiode represents the intensity of the combined beams, which is dependent on the phase difference between the incident right arm and the reflected left arm plus the phase of the grating pattern. The phase difference between the incident right arm and the reflected left arm is just the phase error in the fringe locking loop, which is always driven to zero by the controller. Therefore, the phase of the align-

ment grating can be detected by measuring the voltage read-out from the photodiode when moving the stage.

For the heterodyne reading mode [Fig. 2(b)],<sup>11</sup> the left interference arm is modulated by 90 MHz and the right interference arm by 110 MHz. The phase difference between the incident left arm and the incident right arm is detected by phase meter 3. Phase meter 4 detects the phase difference between the back-diffracted left arm and the reflected right arm. As we know, the phase of the back-diffracted left arm is the summation of the phase of the incident left arm and the phase of the grating pattern. Since the reflected right arm has the same phase as the incident right arm, the phase of grating pattern can be calculated by subtracting the measurement of phase meter 3 from the measurement of phase meter 4.

## II. INTERFERENCE FRINGE PHASE CONTROL TECHNIQUE

In spatial-frequency multiplication, one of the most critical tasks is to accurately place subsequent grating patterns with respect to the alignment grating, which is also called phase control of the overlay. In order to fabricate 50 nm pitch patterns with four-factor spatial-frequency multiplication in the future, our overlay objective is to obtain a  $1\sigma$  overlay

FIG. 1. Schematic depiction of the spatial frequency doubling technique.

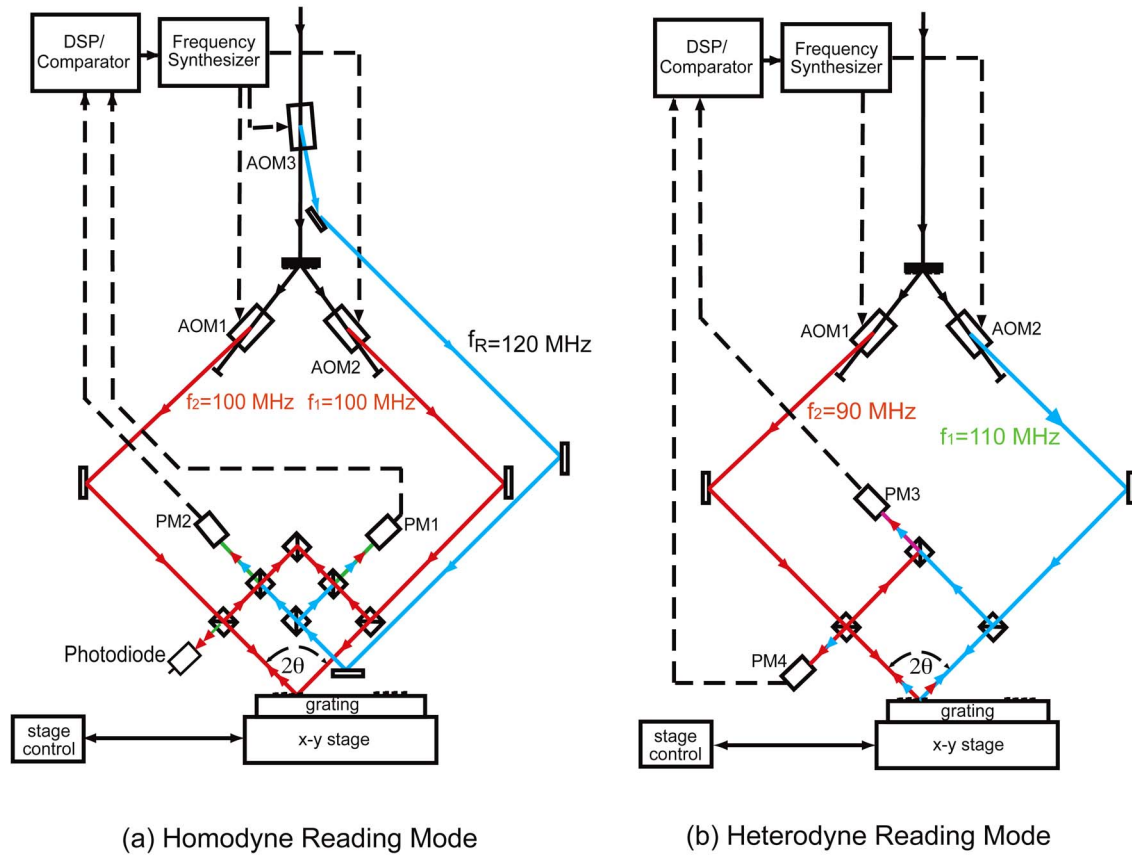


FIG. 2. Homodyne and heterodyne reading modes of the Nanoruler.

error of less than 3 nm. Based on this objective, three key variables (the angle, period, and phase) of the alignment grating are measured with high accuracy and utilized to position subsequent patterns with respect to the alignment grating.

The angle of the alignment grating is utilized to pattern new gratings exactly along the direction of the alignment grating lines. The scheme for measuring the angle of the alignment grating is illustrated in Fig. 3. When scanning the interference fringes from point A to B on the substrate, which

is performed by moving the stage holding the substrate, the phase variation between two points is measured in the homodyne reading mode. The angle  $\theta$  between the scan direction and the direction of the alignment grating lines is calculated using Eq. (1), where  $\phi_B$  is the unwrapped grating phase at point B,  $\phi_A$  is the unwrapped grating phase at point A,  $p$  is the period of the alignment grating, and  $K$  is the distance between points A and B,

$$\theta = \frac{\phi_B - \phi_A}{2\pi K} p. \tag{1}$$

Since the scan direction is known, the direction of the alignment grating lines, or the angle of the alignment grating, can be obtained after calculating  $\theta$ . Based on the overlay objective, the angle measurement error should be less than  $0.1 \mu\text{rad}$ , which is dominated by the phase measurement errors at points A and B. By increasing the scanning distance  $K$  (e.g., 30 mm), the required measurement accuracy can be achieved.

The period of grating patterns on the substrate can change by several picometers daily due to thermal expansion or certain wafer processing steps leading to thin film stress. Patterning new gratings using the just-measured period of the alignment grating can mitigate the effect of daily period change. A technique developed by Chen can be employed to measure the period of the alignment grating.<sup>9</sup> As shown in

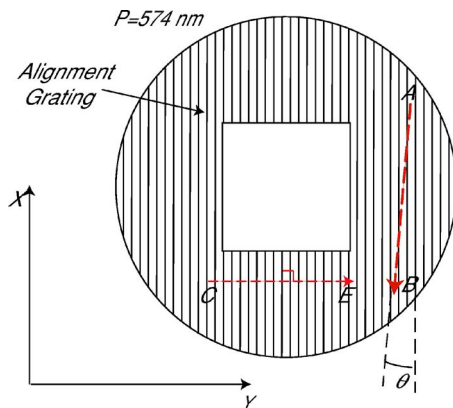
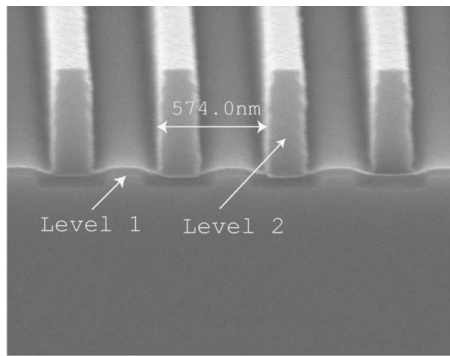
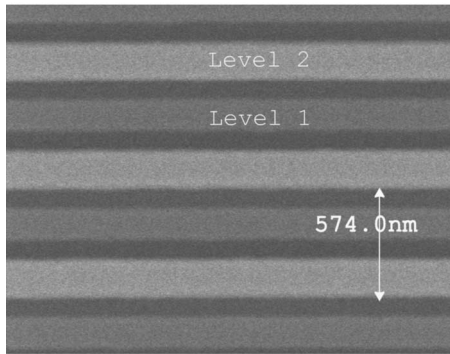


FIG. 3. Schemes for measuring the angle (AB) and period (CE) of the alignment grating.



(a) Cross-section SEM Image



(b) Top-view SEM Image

FIG. 4. Electron micrographs of two-level overlay results. The photoresist is Sumitomo PFI-88 exposed with a wavelength of 351.1 nm.

Fig. 3, we scan the interference fringes on the substrate in a direction perpendicular to the alignment grating lines by a distance  $D$ . Using homodyne reading mode, the phase variation during scanning is measured. The period of the alignment grating  $p$  is given by Eq. (2), where  $\phi_E$  is the unwrapped grating phase at point  $E$  and  $\phi_C$  is the unwrapped grating phase at point  $C$ ,

$$p = \frac{2\pi D}{\phi_E - \phi_C}. \quad (2)$$

The period measurement error is required to be less than 0.06 pm in order to achieve the overlay objective. Following the same method as the angle measurement, increasing the scanning distance  $D$  can achieve the required period measurement accuracy.

In spatial-frequency multiplication, it is critical that subsequent grating patterns have precisely controlled phase shifts relative to the alignment grating in order to insert new grating patterns between previous ones. Before patterning new grating patterns, the relative phase shift between the new grating pattern and the alignment grating is set to a desired value. The Nanoruler is capable of measuring and resetting the phase of the alignment grating in a simple way. The homodyne reading mode provides the phase measurement of the alignment grating, and the interference fringe locking function of the Nanoruler<sup>11</sup> allows us to reset the relative phase between the new grating pattern and the alignment grating by moving the interference fringes with a pre-

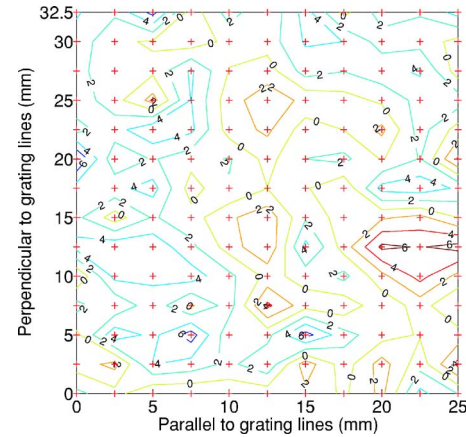


FIG. 5. 2D overlay phase error map (contours in nanometers) with a mean overlay error of  $-1.0 \text{ nm} \pm 2.8 \text{ nm}(1\sigma)$ .

cision of  $2\pi/512$  or about 1.1 nm. The accuracy of grating phase measurement and phase control of the Nanoruler satisfies the overlay requirement.

In order to minimize the alignment grating area, three small gratings could be used instead of a large one. Each grating should have an area no less than the area of the interference image whose diameter is around 1 mm. These gratings should be separately located at any three of four corners of the overlay area. Thus, the minimum area of the alignment grating could be as small as  $3 \text{ mm}^2$ .

### III. RESULTS

In Fig. 4 we show the result of a two-level overlay experiment at a single area of the wafer. We utilized an electron microscope with X-Y automatic stage (Raith 150) to image the overlay area ( $25 \times 32.5 \text{ mm}$ ) with a grid size of 2.5 mm. Based on the micrographs, the overlay phase errors between level 1 and level 2 gratings are calculated. Figure 5 shows a 2D overlay phase error map for a  $25 \times 32.5 \text{ mm}$  area, demonstrating an average overlay error of  $-1.0 \text{ nm}$  with a  $1\sigma$  deviation of 2.8 nm. This level of accuracy should allow the fabrication of 50 nm pitch gratings via four-factor spatial-frequency multiplication starting from a period of 200 nm in the future.

### IV. MAIN FACTORS IMPAIRING THE OVERLAY ACCURACY

The main factors impairing the overlay accuracy are particle-induced substrate distortion and any nonlinear distortion of the alignment grating. In this section the effects of these factors are discussed and some techniques are described to minimize the corresponding effects.

#### A. Particle-induced substrate distortion

Any sizable particle trapped between the back surface of the substrate and the chuck surface will cause in-plane distortion of the substrate,<sup>10</sup> which results in measurement errors of the key variables (the angle, period, and phase) of the alignment grating, and results in the nonlinear distortion of

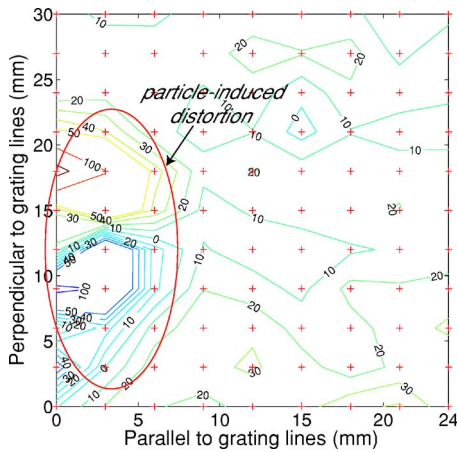


FIG. 6. 2D overlay phase error map (contours in nanometers) demonstrating particle-induced distortion.

grating patterns. The particle effect on the overlay is demonstrated in Fig. 6. Note that one particle trapped during the level 1 pattern exposure causes huge overlay phase errors (peak-to-valley error is more than 200 nm) over a large area. Improvement in the cleaning of the back surface of the substrate and the chuck surface can decrease the number of particles and limit the particle size, which can reduce the particle effect to some extent. A vacuum pin chuck<sup>12</sup> is an alternative to minimize the particle problem.

## B. Nonlinear distortion of the alignment grating

Nonlinear distortion of the alignment grating, which is mainly caused by particles between the substrate and the chuck during patterning of the alignment grating, will result in measured values of the angle, period, and phase that differ from those of the undistorted alignment grating. Local distortions of the alignment grating at start and end locations of the measurements for angle and period will cause errors in the measurement of the corresponding unwrapped grating phases and thus induce errors in the angle and period measurements. When measuring and resetting the phase of the alignment grating for the level 1 and level 2 patterns, if the local distortion at the measurement location for the level 1 pattern is different from that for the level 2 pattern, which easily occurs since the repositioning accuracy of the substrate is only 1~2 mm, a constant overlay phase error over the whole overlay area will be introduced. The heterodyne reading mode provides an easy way to make a 2D phase map of the alignment grating. Based on the phase map, nondis-

torted areas of the alignment grating can be selected to take the angle, period, and phase measurements and thereby avoid errors due to nonlinear distortions.

## V. CONCLUSION AND FUTURE PLANS

In this paper a phase control technique for accurately overlaying interference lithography exposures has been developed. The factors impairing phase control have been identified and corresponding approaches have been developed to minimize their impacts. Based on the phase control technique, doubling the spatial frequency of a 574 nm pitch grating pattern has been achieved over a  $25 \times 32.5$  mm<sup>2</sup> area with an average overlay error of  $-1.0$  nm and a  $1\sigma$  deviation of 2.8 nm. In the future, we hope to perform four-factor spatial-frequency multiplication starting with a principal pitch of 200 nm. We believe the practical limit of this phase control technique is mainly due to the accuracy of the stage interferometry.

## ACKNOWLEDGMENTS

The authors gratefully acknowledge the assistance of Robert Fleming from the MIT Space Nanotechnology Laboratory. This research is support by the National Science Foundation under the Nanoscale Interdisciplinary Research Team (NIRT) Grant DMI-0506898.

- <sup>1</sup>R. K. Heilmann, C. G. Chen, P. T. Konkola and M. L. Schattenburg, *Nanotechnology* **15**, S504 (2004).
- <sup>2</sup>S. R. J. Brueck, "Optical and Interferometric Lithography—Nanotechnology Enablers," in *Proceedings of the IEEE*, Oct. 2005, Vol. 93, p. 10.
- <sup>3</sup>D. C. Flanders, A. M. Hawryluk, and H. I. Smith, *J. Vac. Sci. Technol.* **16**, 1949 (1979).
- <sup>4</sup>A. M. Hawryluk and H. I. Smith, *Opt. Lett.* **7**, 402 (1982).
- <sup>5</sup>B. Cui, Z. Yu, H. Ge, and S. Y. Chou, *Appl. Phys. Lett.* **90**, 043118 (2007).
- <sup>6</sup>Z. Yu, W. Wu, L. Chen, and S. Y. Chou, *J. Vac. Sci. Technol. B* **19**, 2816 (2001).
- <sup>7</sup>S. H. Zaidi and S. R. J. Brueck, *Proc. SPIE* **3676**, 371 (1999).
- <sup>8</sup>A. A. Freschi, F. J. dos Santos, E. L. Rigon, and L. Cescato, *Opt. Commun.* **208**, 41 (2002).
- <sup>9</sup>C. G. Chen, "Beam alignment and image metrology for scanning beam interference lithography—Fabricating gratings with nanometer phase accuracy," Ph.D. dissertation, Massachusetts Institute of Technology, June 2003.
- <sup>10</sup>P. T. Konkola, "Design and analysis of a scanning beam interference lithography system for patterning gratings with nanometer-level distortions," Ph.D. dissertation, Massachusetts Institute of Technology, June 2003.
- <sup>11</sup>R. K. Heilmann, P. T. Konkola, C. G. Chen, G. S. Pati, and M. L. Schattenburg, *J. Vac. Sci. Technol. B* **19**, 2342 (2001).
- <sup>12</sup>A. Une, P. Konyoo, M. Mochida, K. Yoshitomi, and S. Matsui, *Microelectron. Eng.* **61–62**, 113 (2002).